

## Subproject E4.01

# Super-Resolution Optical Microscopy

**Principal Investigator: G. Ulrich Nienhaus**

**CFN-Financed Scientists: N. Azadfar (1/2 TV-L E13, 2 months), S. Brandholt (3/4 TV-L E13, 3 months, 2/3 TV-L E13, 3 months), G. Chen (TV-L E13, 4 months), R. Dörlich (3/4 TV-L E13, 7 months), J. Fuchs (1/2 TV-L E13, 3 months), S. Gayda (3/4 TV-L E13, 15 months), A. Kobitski (1/2 TV-L E13, 6 months), E. Nickel (3/4 TV-L E13, 3 months), R. Rieger (3/4 TV-L E13, 3 months, 1/2 TV-L E13, 12 months), H. Sielaff (TV-L E13, 11.5 months).**

**Further Scientists: Dr. Michael Herrmann, Dr. Karin Nienhaus.**

**Institut für Angewandte Physik  
Karlsruher Institut für Technologie (KIT)**

## Super-Resolution Optical Microscopy

### Introduction and Summary

Light microscopy is arguably the most important technique for the study of living systems because it allows cells and tissues to be imaged in all three spatial dimensions over extended periods of time under minimally invasive, close-to physiological conditions. Conventional light-optical microscopy is diffraction-limited and, hence, only structures larger than  $\sim 200$  nm can be resolved. Given that typical biological macromolecules have extensions of only a few nanometers, there is considerable need for imaging techniques with nanoscale spatial resolution. Electron microscopy is a well-established, powerful method for high-resolution imaging of biological samples, but the requirement for high vacuum, often combined with low temperature, restricts its application to fixed specimens. For live-cell imaging, there is no alternative to optical microscopy. Recent years have witnessed the emergence of several advanced optical microscopy concepts that either fully exploit the power of diffraction-limited microscopy, including confocal laser scanning microscopy (CLSM), structured illumination microscopy (SIM), 4Pi microscopy, total internal reflection fluorescence microscopy (TIRFM) or circumvent the resolution limit, including photoactivation localization microscopy (PALM, FPALM, STORM) [1-3], saturable optical fluorescent transition (RESOLFT, STED) microscopy [4, 5], saturated SIM (SSIM) [6, 7] and super-resolution optical fluctuation imaging (SOFI) [8]. With spatial resolutions in the range 10 – 50 nm, these super-resolution methods narrow the resolution gap between light and electron microscopy significantly and satisfy the growing demand for higher resolution in live-cell imaging.

To investigate physiological processes in living cells, tissues and organisms, it does not suffice to spatially resolve biological structures on the nanoscale; we also need to monitor their development in time. Naturally, the enhanced information content of super-resolution imaging comes at the expense of speed. Therefore, many researchers including ourselves are presently trying to optimize super-resolution imaging so as to accelerate image acquisition. However, specialized techniques have also been developed for the study of fast dynamics using optical microscopy. Especially fluctuation correlation experiments, in principle, offer a time resolution down to the microsecond region. These techniques can be applied to raster images of, e.g., entire cells (raster image correlation spectroscopy, RICS [9]), or one can probe dynamics locally in a tiny focal volume placed, e.g., inside a living cell, by fluorescence correlation spectroscopy (FCS) [10]. Förster resonance energy transfer (FRET) enables us to measure biomolecular interactions and conformational changes with nanometer accuracy on sub-millisecond time scales. While quantitative fluorescence microscopy experiments on cells and tissues are often revealing from a biological point of view, the techniques are also powerful for the study of purified biomolecular samples under well-controlled conditions. Explorations of structure-dynamics-function relationships of biological macromolecules and their mutual interactions are essential for the understanding of processes occurring in the much more complex cellular environment. Consequently, we frequently employ fluorescence-based techniques to first probe the dynamics of individual biomolecules, proteins and nucleic acids, in an aqueous solvent

environment at a well-defined pH and at physiological temperatures. In a second step, these measurements may be transferred into the living cell.

In project E 4.01, the main aim is to further extend both the spatial and temporal resolution of optical imaging techniques to enable the analysis of molecular interactions in space and time in living cells. Here we focus primarily on nanobiology applications, however, our tools and techniques are widely applicable to nanoscience in general. Specifically, we develop and apply

- super-resolution methods of optical imaging including PALM and STED,
- FRET techniques to observe conformational changes on the nanometer scale in vitro and in vivo,
- methods to study biomolecular dynamics, involving correlation approaches (FCS, RICS),
- quantitative tools for image processing and analysis,
- advanced luminescent markers for super-resolution optical imaging (engineering of fluorescent proteins, semiconductor and metal cluster nanoparticles) and spectroscopic/microscopic tools for their characterization.

The principal investigator, G. U. Nienhaus, has joined the faculty of KIT on April 16, 2009. Part of the laboratory equipment was transferred from the University of Ulm to KIT in 2009 and put back into operation mainly in laboratories in the CFN building. In the meantime, new equipment has been acquired with start-up funds from KIT and CFN, and expansion of the facilities is presently ongoing.

Since 2009, subproject E4.01 has led to 29 publications altogether. Among these are 1 article in *Nature Nanotechnology*, 2 in *Nature Methods*, 1 in *J. Clin. Invest.*, 1 in *Blood*, 2 in *EMBO J.*, 3 in *JACS*, 2 in *ACS Nano*, 2 in *Biomaterials*, and 2 in *Small*.

## 1. Super-resolution Optical Imaging at the CFN

The detection of spatially and temporally regulated molecular events in living cells, tissues and organisms is of utmost importance for achieving a better understanding of biological function. Therefore, it is necessary to extend both the spatial and temporal resolution of optical imaging techniques (for a concise review on the techniques, see [E4.01:15]). In our work, we focus mainly on PALM, STED and confocal microscopy including two-photon excitation and 4Pi detection with two opposing objective lenses.

Photoactivation localization microscopy (PALM) is a wide-field technique based on the detection of the emission from individual fluorophores. Importantly, these emitters must be photoactivatable by irradiation with visible light. By activating them sparsely and stochastically, each CCD camera frame contains only a few spots of the size of the point spread function, which allows each molecule to be precisely localized (Fig. 1 a).

We have built a PALM system as a wide-field microscope with multiple laser lines at the CFN. It can also be used as a TIRF microscope with excitation through the objective lens ('objective

type' TIRF). The images are collected with a highly-sensitive EMCCD camera (Andor Ixon 897D) with 35 frames per second (fps) in two color channels by using an image splitter. In addition, we have recently added a high speed camera (Andor Ixon 860D) in combination with an image splitter (Cairn Research Optosplit II), which allows us to take image sequences in excess of 500 fps. Simultaneous (instead of sequential) image acquisition in the two color channels by using an image splitter or, alternatively, two synchronized cameras, avoids channel mismatches due to cellular dynamics. Further hardware developments are ongoing, including three-dimensional PALM image acquisition.

We are especially interested in applying super-resolution PALM to live cells and, therefore, have installed a live-cell incubation chamber (Pecon Incubator XL dark), which allows us to image mammalian cells over extended periods of time at 37°C under controlled humidity and CO<sub>2</sub> atmosphere.

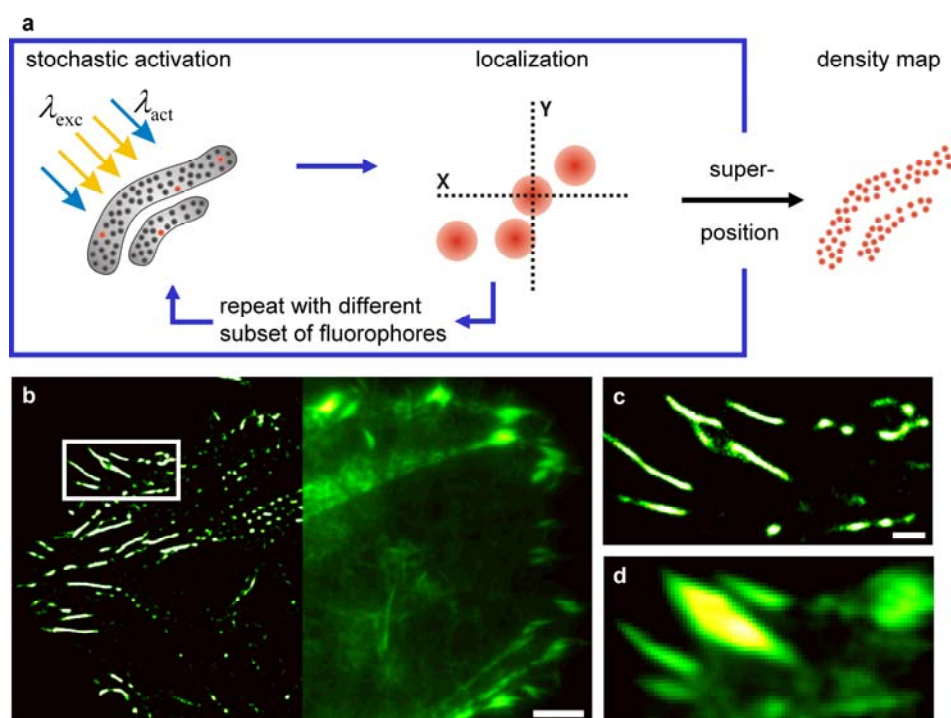


Fig. 1. Photoactivation localization microscopy (PALM). (a) Schematic depiction of the principle. (b) Standard total internal reflection (TIRF) microscopy image (right) and PALM image reconstruction (left) of the microfilament network of a live HeLa cell expressing an  $\alpha$ -actinin-mIrisFP fusion protein, scale bar, 5  $\mu\text{m}$ . (c, d) Close-ups of the region marked by the white frame in (b) imaged by (c) PALM and (d) TIRFM, scale bar, 1  $\mu\text{m}$ .

Super-resolution PALM images are reconstructed by localizing typically 10 – 100 individual molecules in each of several hundred to thousand image frames. To keep up with cell locomotion, an individual PALM image must be collected within a time interval short enough so

that features have not moved appreciably (i.e., more than the desired resolution). Currently, we acquire PALM images on the second to minute time scale, the fastest speed being offered by the new high-speed camera. With our own photoactivatable proteins, we routinely achieve image resolutions in the range 20 – 30 nm in live-cell imaging applications (Fig. 1 b-d). In Fig. 2, we present another example of live-cell imaging, showing that reconfiguration of the microtubular network of a HeLa cell can be tracked by measuring PALM images with an overall frame time of 27 s.

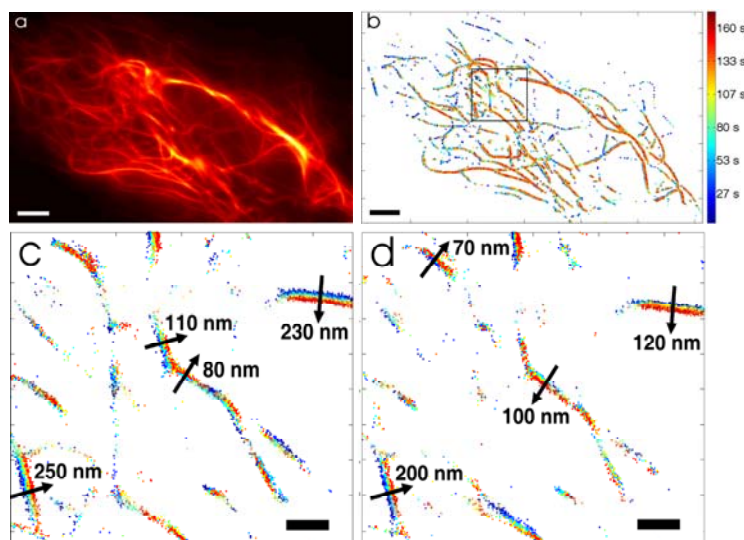


Fig. 2. Microtubules of a live HeLa cell, visualized by the tubulin-binding fusion protein Rita-mcavFP. Image acquisition: 1600 individual frames, 100 ms each. (a) Overall TIRFM image, (b) position plot, individual fluorophores color-coded according to their time of detection. (c) Expanded view of the region marked by the black frame in (b) shows cellular dynamics during data collection that leads to an additional blurring of the high-resolution image, (d) same region as in (c), but 5 min later.

In stimulated emission depletion (STED) microscopy, the focused fluorescence excitation beam, with a diffraction-limited, near-Gaussian shape is overlaid spatially with a red-shifted depletion beam that again deexcites the molecules by stimulated emission. By using a suitable phase plate, the focused STED beam acquires an annular shape, featuring zero intensity in the center. Thus, only molecules in the center of the Gaussian excitation spot are not deexcited by the STED beam. By appropriate adjustment of the power of the STED beam, the emission can be confined to a few molecules close to the center of the excitation beam (Fig. 3 a). Raster-scanning of the STED-sharpened beam and the sample relative to each other yields images with a resolution below the diffraction barrier (Fig. 3 b).

Over the past few months, we have built a STED set-up in our lab, which we intend to employ especially for STED-FCS. Our STED imaging system is based on a supercontinuum white light laser source (Fianium SC-450-PP-HE) for fluorescence excitation, which provides the two wavelengths (excitation/depletion) needed for a STED microscope. The setup has already been

tested on fluorescent beads and solutions of fluorescent dyes. For investigating live cells, the piezo scanner currently in use on the STED microscope is too slow. Therefore, a fast beam scanner (Till Photonics, Yanus IV Digital Scan Head) will be integrated into our STED system. This device will also enable us to perform RICS for studying fast molecular movements within cells.

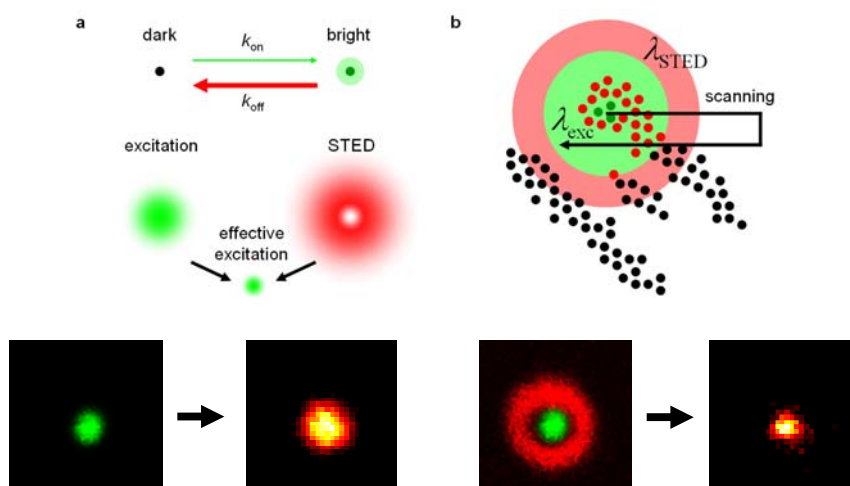


Fig. 3. (a) Schematic depiction of stimulated emission depletion (STED). (b) Sketch of the scanning procedure. (c) Proof of principle: The image of a fluorescent bead (diameter: 100 nm) with the excitation beam is a spot with a width (FWHM) of 470 nm. Application of the STED pulse in addition to the excitation pulse lowers the width to 320 nm.

In addition to our home-built super-resolution devices, we develop and operate slow-scanning CLSMs especially designed for single-molecule (FRET) detection. Moreover, we operate a commercial Leica TCS 4Pi CLSM in our laboratory. By using two-photon excitation and 4Pi detection with two opposing objective lenses in an interferometric design, it provides an axial resolution of  $\sim 100$  nm and, thus, an  $\sim 5 - 7$ -fold improvement over standard CLSM. This property makes this microscope particularly useful for acquiring 3D stacks of cells. Fig. 4 shows images of *E. coli* cells imaged in standard confocal and 4Pi mode for comparison.

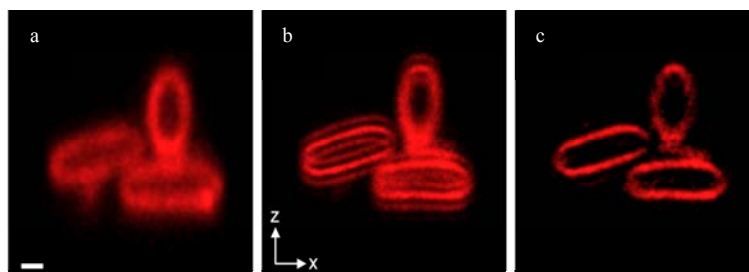


Fig. 4. (a) Confocal image of membrane-stained (*DiI*) *E. coli* bacteria; scale bar, 500 nm. (b) Raw 4Pi image of the same specimen in the x-z plane showing the superior resolution in the axial direction. (c) 4Pi image after deconvolution.

Our fluorescence microscopes were employed in a number of collaborative studies with research groups from biology and medicine, for which we contributed with our technical expertise in quantitative fluorescence imaging as well as with marker proteins [E4.01:4, E4.01:28, E4.01:29].

## 2. Quantitative Image Analysis for Localization Microscopy

Localization microscopy is essentially an image processing technique, based on the reconstruction of high-resolution images from a few hundred up to a few thousand CCD camera frames of a wide-field microscope. Each CCD frame contains only a small number of individual fluorescence emitters. Their precise locations are determined to within tens of nanometers by a two-step algorithm. First, peaks corresponding to individual fluorophores are identified within each frame (search step), and, subsequently, their centers of mass are determined (localization step).

For fluorophore localization in PALM image analysis, a full least-squares fit of the point spread function with a Gaussian distribution yields optimal localization precision, but the complete image analysis may take up to several hours on a single CPU [11]. Consequently, the image can only be inspected long after data acquisition, which makes it difficult to optimize data acquisition conditions, e.g., to select optimal activation/excitation intensities and acquisition times. There are two strategies for accelerating image reconstruction that we have both pursued, namely (1) the use of ‘raw computation power’ by largely parallelized computation of the molecule loci, or (2) the use of fast, algebraic localization algorithms that avoid the tedious fitting procedure.

The first strategy can be implemented in a simple manner by using modern graphics processing units (GPUs) instead of the conventional central processing units (CPUs). By implementing a maximum likelihood algorithm on a GPU, we have developed an image reconstruction method that is sufficiently fast for real-time processing of localization images even from the most advanced EMCCD cameras working at full frame rate without compromising localization precision or field of view [E4.01:24].

We have also developed a fast PALM image reconstruction software based on the algebraic fluoroBancroft algorithm, which exploits the fact that the intensity captured within each image pixel depends on the distance from the point source [E4.01:6]. The position of the source can thus be calculated from the measured intensities of the pixels associated with this source; no data fitting is required. The localization procedure resembles the one used for the global positioning system (GPS). An instant high-resolution preview is thus available, making the data acquisition procedure more intuitive and interactive. The minor resolution loss of the fluoroBancroft algorithm (Fig. 5) is by far outbalanced by the ‘what you see is what you get’ advantage during data acquisition. The raw image data are still available for subsequent offline analysis.

Our online software for PALM image analysis not only enables more efficient cellular imaging experiments, but also offers the possibility to automatically adjust key experimental parameters, e.g., the activation laser intensity, thus making the PALM method much more user-friendly.

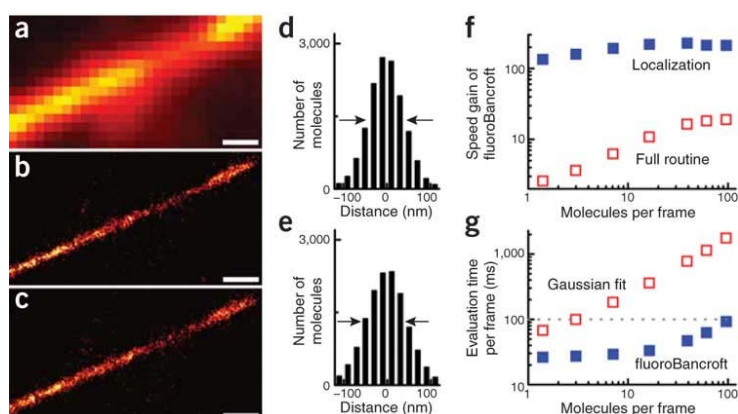


Fig. 5. TIRF microscopy image (a) and PALM images of stress fibers analyzed by Gaussian fit localization (b) and the fluoroBancroft algorithm (c); scale bars, 500 nm. (d, e) Histograms of the distributions of fluorophores around the contour line as determined by Gaussian fit (d) and fluoroBancroft (e) localization. (f, g) Performance of the image analysis routines based on the Gaussian fit and fluoroBancroft algorithms, as a function of the number of fluorophores in each frame.

### 3. Advanced Luminescent Markers for Super-Resolution Optical Imaging

Super-resolution imaging techniques rely on the ability to control the emission of fluorophores by light irradiation. While STED microscopy uses a fundamental physical mechanism, i.e., stimulated emission, all other super-resolution techniques utilize photoactivatable fluorophores. These should be bright in their activated states, i.e., feature both large fluorescence quantum yields and extinction coefficients to produce strong signals above background, and they should be preferentially non-fluorescent when deactivated. Super-resolution microscopy has been implemented with (1) synthetic fluorophores that can be photoactivated in the presence of thiol-containing reagents, (2) photoactivatable fluorescent proteins, or (3) nanocrystals that show intermittency in their luminescence emission.

Our group has a long-standing research activity in protein structure-dynamics-function studies using (time-resolved) optical and infrared spectroscopy in combination with x-ray crystallography. Recombinant protein expression and protein engineering is essential for this work, and we have set up a biochemistry laboratory in the CFN building for this purpose. Our spectroscopy equipment has permitted the characterization of optical properties not only of proteins [E4.01:10, E4.01:21, E4.01:22], but also of nanocrystals [E4.01:5, E4.01:25] and other nanostructures [E4.01:14]. The in-depth analysis of structure-dynamics-function relationships in a wide variety of fluorescent proteins [E4.01:1, E4.01:2, E4.01:3, E4.01:9, E4.01:12, E4.01:20] has enabled us to design optimized variants that are widely used as marker proteins for super-resolution live-cell imaging.

Photoactivatable fluorescent proteins are popular markers for super-resolution imaging, especially for studies in living cells and organisms because they are genetically encoded and thus

produced by the systems under study themselves; no labeling steps are required. Typically, these proteins either show reversible photoactivation between a bright and a dark state, also known as photoswitching, or irreversible photoactivation, also known as photoconversion, which involves a permanent photochemical modification of the fluorescent protein. In 2004, we introduced EosFP, a green-red photoconverting protein, variants of which are currently the brightest fluorescent proteins for PALM imaging [12]. In 2008, we discovered a variant of EosFP, called IrisFP, which combines the two photoactivation modes: It is a photoswitchable green fluorescent protein and, after photoconversion with 400 nm light, again photoswitchable in the red [13]. The physical basis of these changes was elucidated by a combination of optical spectroscopy, x-ray crystallography and molecular (QM/MM) computations. All GFP-like fluorescent proteins are shaped in the form of a cylinder, in which the fluorescent chromophore is generated autocatalytically. In Fig. 6, the four distinguishable states of the IrisFP fluorophore are depicted. Photoswitching is based on a light-driven interconversion between a fluorescent cis state of the chromophore and a non-fluorescent trans state. Green-to-red photoconversion, by contrast, relies on a photo-chemically induced extension of the fluorophore.

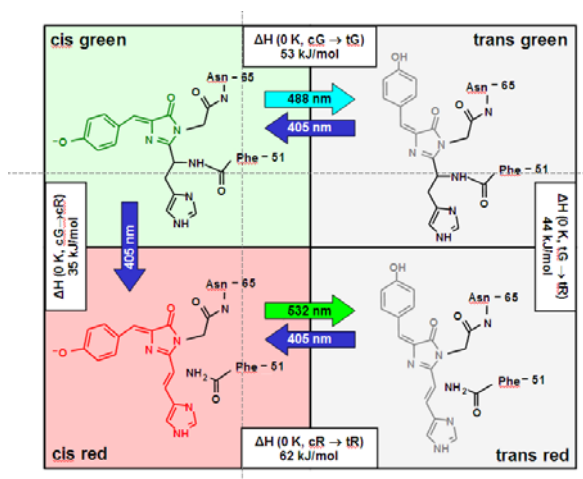


Fig. 6. Photo-induced transformations in IrisFP. Colored arrows represent wavelength to achieve photoactivation. cG: cis-green Iris; tG: trans-green Iris; cR: cis-red Iris; tR: trans-red Iris. Also indicated are the enthalpy differences between the species from quantum-chemical (QM/MM) calculations.

Because the tetrameric nature of IrisFP typically creates problems in fusion protein applications, we have recently developed an advanced, monomeric version denoted as mIrisFP. It has a total of five additional amino acid substitutions with respect to a monomerized EosFP variant. It has excellent expression yield at 37°C and offers the full photoactivation functionality of IrisFP. Its multiple photoactivation modes allow life sciences researchers to perform entirely new experiments, e.g., pulse-chase experiments with sub-diffraction resolution in living cells by using dual-color PALM imaging [E4.01:13].

We have also synthesized and utilized nanocrystals as luminescent labels for imaging applications. Specifically, we have prepared highly luminescent, water-soluble semiconductor core-shell nanoparticles (CdSe/ZnS) with excellent colloidal stability due to zwitterionic stabilizing ligands [E4.01:5]. These and other nanoparticles were extensively used in experiments aimed at exploring interactions between nanoparticles and living matter (see below). Recently, we have also started to explore small, water soluble gold nanoclusters as markers for advanced fluorescence microscopy.

#### 4. Nanoscale Dynamics Studies by Förster Resonance Energy Transfer (FRET)

All life-sustaining processes in a cell are based on intricate, tightly controlled interactions between a vast number of (bio-)molecules. The development of super-resolution optical imaging techniques is driven by the need to observe these nanoscale objects, preferentially in the living cell. In functional processes, conformational changes occur within the biomolecules themselves, and some of these are accessible by using fluorescence microscopy. Analysis of Förster resonance energy transfer (FRET) between two dye molecules specifically attached to a biomolecule of interest, measured at the level of individual biomolecules, has proven to be a particularly powerful approach for the study of structural rearrangements with high temporal and spatial resolution. We have studied molecular motions in RNA [E4.01:7, E4.04:23] and protein molecules [E4.01:27] by using FRET. In the following, we briefly sketch a protein folding study as an example.

Protein folding is one of the most intriguing processes in molecular biophysics. A complete understanding of the mechanisms by which a protein finds its properly folded, functionally competent three-dimensional structure requires a detailed knowledge of the conformational energy landscape governing a multitude of microscopic trajectories by which a polypeptide chain can migrate from the huge number of unfolded conformations to the comparatively well-defined folded state [14, 15].

In previous smFRET (single-molecule FRET) studies, we had investigated the structure and dynamics of surface-immobilized RNase H in the presence of the chemical denaturant GdmCl [16]. RNase H is known to be a typical three-state folder, which transiently populates a partially folded intermediate state during folding in ensemble experiments. However, smFRET experiments revealed only two distinct populations, which were assigned to the folded and unfolded states. A separate intermediate state was not evident from the FRET data, suggesting that it is either spectroscopically not well distinguishable from the other two states or only weakly populated in equilibrium. To resolve this conundrum, we revisited the folding of RNase H. By taking data with excellent statistics and applying a global fitting procedure to FRET histograms at all GdmCl concentrations, in which a number of parameters were constrained, we were able to pin down the hidden intermediate state. The analysis resolved the apparent discrepancy with the bulk data on RNase H and yielded precise free energy differences between the three states. This work forms the basis for future experiments focused on the time dependence of the folding trajectories.

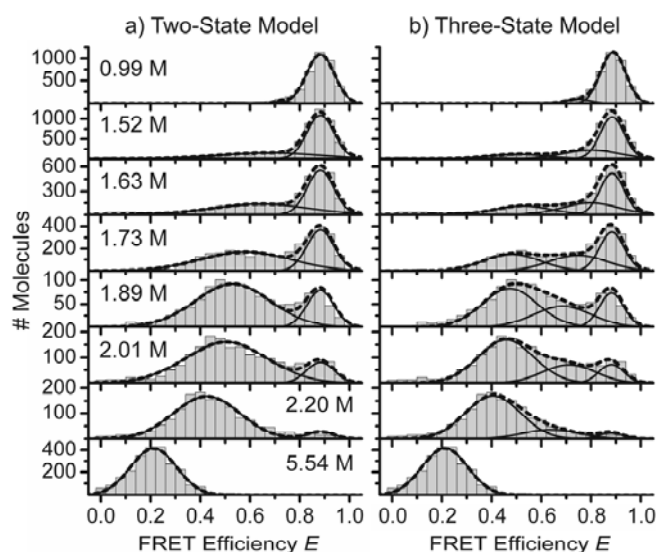


Fig. 7. FRET efficiency histograms from burst analyses of the fluorescence emission from FRET-pair labeled RNase H. a) Two-state analysis. b) Three-state analysis with an additional folding intermediate.

## 5. Methods to Study Biomolecular Dynamics: FCS, 2fFCS, RICS.

Direct optical imaging of fast dynamics in cells is currently limited to a few milliseconds by CCD camera frame times. However, many interesting processes, e.g., intracellular transport or biomolecular interactions require a higher temporal resolution. To study faster dynamics, one may use single-particle tracking instead of scanning entire images with a confocal setup. Alternatively, one can measure time correlations at fixed or slowly varying positions by fluorescence correlation spectroscopy (FCS) and related techniques. Alternatively, one can also analyze confocal images by raster image correlation spectroscopy (RICS) [9], recognizing that raster-scanning imposes a time structure, so that changes in intensity between consecutive points, lines and entire images can be analyzed to yield information on molecular movements.

FCS is a widely used technique to characterize the dynamics of fluorescent species, e.g., single fluorescence emitters in solution and nanostructured environments [17]. In recent years, the technique has found increasing application in live-cell experiments [10]. The measured fluorescence intensity fluctuations (due to diffusion, (photo-)physics or (photo-)chemistry, aggregation, etc.) are analyzed by autocorrelation. FCS yields quantitative information such as diffusion coefficients, hydrodynamic radii, average concentrations or chemical reaction rates.

We have used FCS to precisely monitor the adsorption of serum proteins onto small (10 – 20 nm in diameter) polymer-coated FePt and CdSe/ZnS nanoparticles [E4.01:11, E4.01:18]. The FCS analysis revealed that the proteins form a monolayer, which, for human serum albumine, has a thickness of 3.3 nm. Proteins bind to the negatively charged nanoparticles with micromolar affinity, and time-resolved fluorescence quenching experiments showed that they reside on the

particle for  $\sim 100$  s. These new findings have contributed to our quantitative understanding of the protein corona enshrouding the nanoparticle, which is of utmost importance for the safe application of nanoscale objects in living organisms. These studies were complemented by fast confocal (spinning disk) imaging of nanoparticle endocytosis by living cells to understand the mechanistic details of this process [E4.01:8, E4.01:17, E4.01:19, E4.01:26].

Although FCS can detect changes in particle size in the nanometer range very reliably, it always requires a non-trivial calibration procedure. An advanced version, two-focus-FCS (2fFCS), measures absolute values of diffusion coefficients by introducing an intrinsic, absolute length scale in the measurement. This external ruler is realized by generating two laterally shifted but overlapping laser foci at a fixed and known distance. The analysis rests on the autocorrelation and the cross-correlation of the intensities from the two foci, yielding accurate diffusion coefficients. We have implemented 2fFCS capabilities, and we have also evaluated RICS analysis in recent months.

## 6. Fabrication of Micro- and Nanoscale Structures for Optical Microscopy

Optical imaging experiments on biomolecules, cells and tissues can greatly benefit from micro- and nanostructured devices. They may allow specific optical phenomena to be exploited, such as surface plasmon enhancement of light absorption and scattering, or light confinement by zero-mode waveguides. Other devices may enable the precise control of the environment, including fast mixing and exchange of solvents in single-molecule as well as cellular experiments. We have begun to utilize the nanostructuring facilities at the CFN for preparing zero-mode waveguides, which will allow us to confine the detection volumes of our microscopes to the zepto-liter range, which will be crucial for extending single molecule experiments to more weakly interacting systems. We have already fabricated masks that will be used to generate zero-mode wave guides.

We have also developed lab-on-the-chip devices that allow fast mixing and exchange of solvents. A first application will be protein folding, where fast events typically occur on the microsecond time scale. Changing denaturant concentration is an attractive method to trigger folding (see above). For fast mixing of protein and denaturant, we have microfabricated fluidic systems in polydimethylsiloxane (PDMS), which allow mixing dead times of typically 10  $\mu$ s. To study single molecules in solution, these devices feature very low rates of laminar flow to achieve a sufficiently long residence time of each molecule in the detection volume, i.e., the focal spot of a confocal microscope.

We went through multiple rounds of modification to optimize fluid mixers for single molecule observation. The exit channel leading away from the mixing chamber was made rather wide to decrease the flow speed and, thus, increase the dwell time of the molecules in the detection volume. The length of the feed lines was increased considerably to generate flow resistance, which decreases the sensitivity of the flow rates to small, external pressure perturbations. To avoid protein adsorption onto the device walls, we coated all surfaces in contact with the sample solution with PDMS. To minimize fluorophore photobleaching, which often involves a reaction

with molecular oxygen, additional ‘nitrogen’ channels were included to replace the atmospheric oxygen by nitrogen. The pumping system has to maintain extremely low and steady flow rates in the microliter-per-minute range. Syringe pumps appeared initially promising but produced a pulsating flow pattern at low flow rates. We also tried electro-osmotic pumps, which have no moving parts, but formation of gas bubbles due to their electrolytic activity changed the flow rate over time. In the end, simple hydrostatic pumping turned out to be best suited for our experiments, although achieving long-term stability remains challenging.

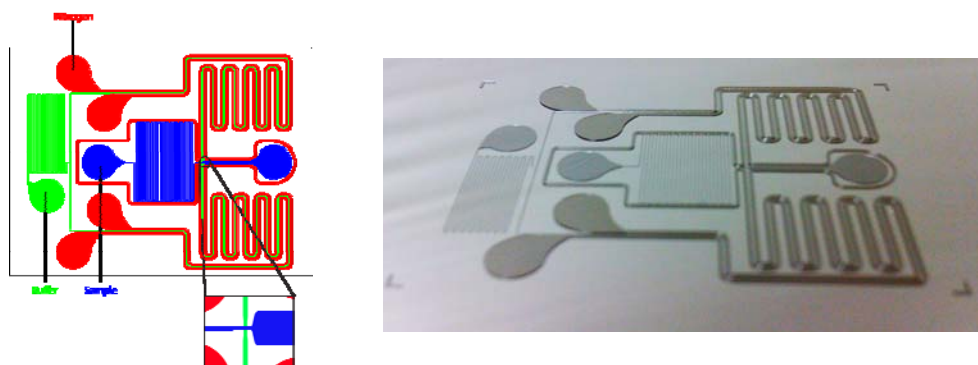


Fig. 8. Schematic and actual realization of a microfluidic mixer for use in single-molecule fluorescence microscopy.

## References

- own work with complete titles -

1. Betzig, E., Patterson, G. H., Sougrat, R., Lindwasser, O. W., *Science* **313** (2006) 1642-1645.
2. Hess, S. T., Girirajan, T. P., & Mason, M. D., *Biophys. J.* **91** (2006) 4258-4272.
3. Rust, M. J., Bates, M., & Zhuang, X., *Nat. Methods* **3** (2006) 793-795.
4. Hell, S. W., *Nat. Methods* **6** (2009) 24-32.
5. Hell, S. W., *Science* **316** (2007) 1153-1158.
6. Gustafsson, M. G., *Proc. Natl. Acad. Sci. U S A* **102** (2005) 13081-13086.
7. Heintzmann, R., & Gustafsson, M. G., *Nature Photonics* **3** (2009) 362-364.
8. Dertinger, T., Colyer, R., Iyer, G., Weiss, S., & Enderlein, J., *Proc. Natl. Acad. Sci. U S A* **106** (2009) 22287-22292.
9. Rossow, M. J., Sasaki, J. M., Digman, M. A., & Gratton, E., *Nat. Protoc.* **5** (2010) 1761-1774.
10. Yu, S. R., Burkhardt, M., Nowak, M., Ries, J., Petrasek, Z., Scholpp, S., Schwille, P., & Brand, M., *Nature* **461** (2009) 533-536.
11. Gould, T. J., Verkhusha, V. V., & Hess, S. T., *Nat. Protoc.* **4** (2009) 291-308.

12. Nienhaus, K., Nienhaus, G. U., Wiedenmann, J., & Nar, H., Structural basis for photo-induced protein cleavage and green-to-red conversion of fluorescent protein EosFP, *Proc. Natl. Acad. Sci. U S A* **102** (2005) 9156-9159.
13. Adam, V., Lelimosin, M., Boehme, S., Desfonds, G., Nienhaus, K., Field, M. J., Wiedenmann, J., McSweeney, S., Nienhaus, G. U., & Bourgeois, D., Structural characterization of IrisFP, an optical highlighter undergoing multiple photo-induced transformations, *Proc. Natl. Acad. Sci. U S A* **105** (2008) 18343-18348.
14. Lipman, E. A., Schuler, B., Bakajin, O., & Eaton, W. A., *Science* **301** (2003) 1233-1235.
15. Cecconi, C., Shank, E. A., Bustamante, C., & Marqusee, S., *Science* **309** (2005) 2057-2060.
16. Kuzmenkina, E. V., Heyes, C. D., & Nienhaus, G. U., Single-molecule Förster resonance energy transfer study of protein dynamics under denaturing conditions, *Proc. Natl. Acad. Sci. U S A* **102** (2005) 15471-15476.
17. Haustein, E., & Schwille, P., *Annu. Rev. Biophys. Biomol. Struct.* **36** (2007) 151-169.